p38 MAPK-dependent shaping of the keratin cytoskeleton in cultured cells

Stefan Wöll, Reinhard Windoffer, and Rudolf E. Leube

Department of Anatomy and Cell Biology, Johannes Gutenberg University, 55128 Mainz, Germany

Plasticity of the resilient keratin intermediate filament cytoskeleton is an important prerequisite for epithelial tissue homeostasis. Here, the contribution of stress-activated p38 MAPK to keratin network organization was examined in cultured cells. It was observed that phosphorylated p38 colocalized with keratin granules that were rapidly formed in response to orthovanadate. The same $p38^{P}$ recruitment was noted during mitosis, in various stress situations and in cells producing mutant keratins. In all these situations keratin 8 became phosphorylated on S73, a well-known p38 target site. To demonstrate that p38-dependent keratin phosphorylation determines keratin organization, p38 activity was pharmacologically and genetically modulated: up-regulation induced keratin granule formation, whereas down-regulation prevented keratin filament network disassembly. Furthermore, transient p38 inhibition also inhibited keratin filament precursor formation and mutant keratin granule dissolution. Collectively, the rapid and reversible effects of p38 activity on keratin phosphorylation and organization in diverse physiological, stress, and pathological situations identify p38-dependent signalling as a major intermediate filament–regulating pathway.

Introduction

The ubiquitous cytoskeletal 8–12-nm intermediate filaments (IFs) are made of cell type–specific molecular components that are encoded by several multigene families encompassing at least 71 functional genes in human (Herrmann et al., 2003; Omary et al., 2004; Schweizer et al., 2006). The largest subfamilies are the type I and type II keratins in epithelial cells, which are obligatory heteropolymers contributing equally to mature keratin filaments (KFs) by forming stable double-stranded coiled-coil heterodimers (Herrmann et al., 2003). KFs provide mechanical stability and overall resilience for epithelial tissues (Coulombe and Omary, 2002; Magin et al., 2007). They are organized in different ways in the various epithelial cell types, generating thick bundles in epidermal keratinocytes, apically restricted and densely woven mats in enterocytes, subplasmalemmal enrichments in hepatocytes, or finely dispersed three-dimensional networks in several cultured epithelial cell types. These alternative arrangements in combination with the diverse cell shapes that are required in living tissues suggest that the KF cytoskeleton is highly dynamic. Two types of regulation are being considered: differential association of KFs with scaffolding proteins and keratin modification (Coulombe and Omary, 2002; Coulombe and Wong, 2004). A scaffolding function is apparently provided by cell adhesion structures, and key molecular players have been identified such as the desmosomal plaque proteins desmoplakin/plakophilin/plakoglobin (Hatzfeld and Nachtsheim, 1996; Smith and Fuchs, 1998; Kowalczyk et al., 1999; Hofmann et al., 2000) and the hemidesmosomal components plectin and bullous pemphigoid antigen 1 (Steinbock et al., 2000; Fontao et al., 2003). The multifunctional cytoskeletal crosslinker plectin may also participate in attachment to other cytoskeletal elements and the nucleus (Leung et al., 2002; Rezniczek et al., 2004; Wilhelmsen et al., 2005). In addition, keratin bundling is favored by proteins such as filaggrin (Listwan and Rothnagel, 2004). The importance of protein modification for keratin organization has been widely recognized and phosphorylation is considered to be the major contributing factor (Omary et al., 2006). Because altered phosphorylation is often accompanied by structural changes, it is generally assumed that a cause-and-effect relationship exists between both. In accordance, increased keratin phosphorylation is observed during mitosis and in various stress paradigms, i.e., in situations of considerable keratin reorganization (Liao et al., 1997; Toivola et al., 2002; Ridge et al., 2005). It was further suggested that keratin phosphorylation is the result of antagonistic kinase and phosphatase activities that are regulated in a cell type–specific manner (Tao et al., 2006). Yet, a direct temporal and spatial correlation between specific enzymatic activity,

Correspondence to Rudolf Leube: leube@uni-mainz.de

Abbreviations used in this paper: IF, intermediate filament; K8, keratin 8; KF, keratin filament; OV, orthovanadate; $p38^{P}$, phosphorylated p38.

The online version of this article contains supplemental material.

The Journal of Cell Biology, Vol. 177, No. 5, June 04, 2007 795–807
http://www.jcb.org/cgi/doi/10.1083/jcb.200703174

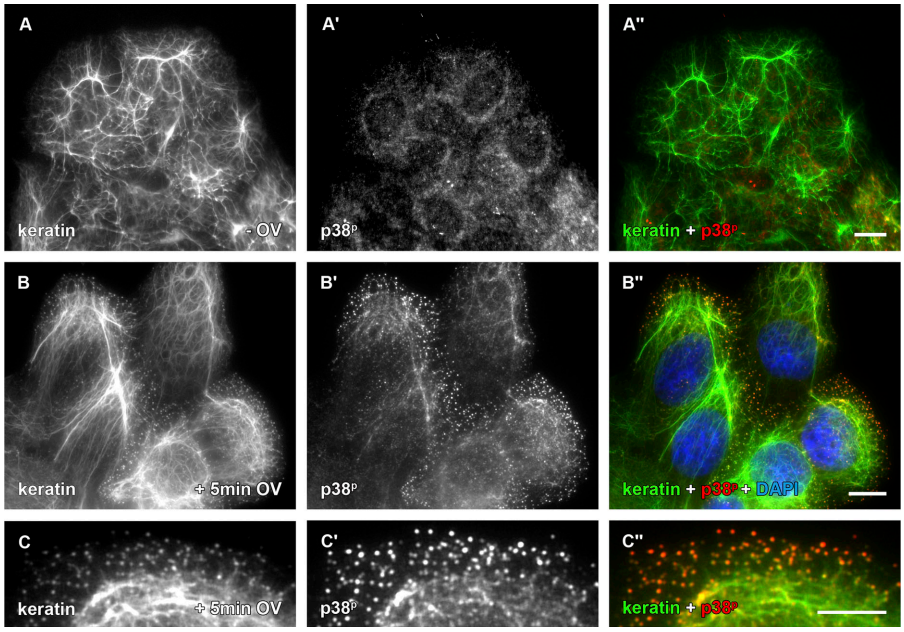

Figure 1. **p38P colocalizes with forming keratin granules in OV-treated cells.** The fluorescence micrographs of methanol/acetone-fixed A431 cells of clone AK13-1 show the distribution of keratin HK13-EGFP (A–C) together with p38P using polyclonal primary antibodies (A′–C′; merge in A″–C″) in the absence (A) and presence of 20 mM OV (B and C). Note that p38P is distributed diffusely in nontreated cells, but colocalizes with keratin granules that are formed in response to OV. Bars, 10 μm.

altered target phosphorylation sites in keratin polypeptides and consecutive keratin reorganization, has not been established so far in the context of a living cell.

To examine direct linkages between kinase/phosphatase activities, keratin modifications, and KF organization, we therefore established epithelial cell culture systems in which we are able to monitor in real time the rapid and reversible orthovanadate (OV)-induced KF network disassembly into keratin granules by live-cell fluorescence microscopy (Strnad et al., 2002). Although overall keratin phosphorylation did not change substantially under these conditions (Strnad et al., 2002), keratin reorganization could be prevented by preincubation with a specific p38 MAPK inhibitor (Strnad et al., 2003). Because p38 is known to phosphorylate keratins (Feng et al., 1999; Ku et al., 2002; Toivola et al., 2002), we decided to analyze the relationship between its activity, modification of keratin target sites, and keratin arrangement in more detail.

Results

OV-induced keratin granules colocalize with p38P and express p38P target sites

We have recently shown that rapid and reversible restructuring of the keratin cytoskeleton occurs in the presence of OV, a well known, yet rather unspecific tyrosine phosphatase inhibitor that also effects other enzymes such as cellular ATPases (Gibbons et al., 1987; Strnad et al., 2002). This reorganization can be effectively prevented by ambient light, and to a lesser degree, by preincubation with the specific p38-inhibitor SB203580 (Strnad et al., 2003). The latter observation suggested that signaling via the p38-MAPK pathway is involved in the regulation of KF organization. To further pursue this idea, we examined the distribution of activated p38 by immunofluorescence microscopy of OV-treated vulva carcinoma-derived AK13-1 cells producing fluorescent HK13-EGFP. Shortly after addition of the drug, a remarkable redistribution of phosphorylated p38 (p38P) from a diffuse cytoplasmic pool lacking colocalization with the keratin system to a marked granular pattern occurred, coinciding with the appearance of keratin granules (Fig. 1). At intermediate stages of KF disassembly remnant, normal-appearing KFs were negative for p38P, whereas thick KF bundles were weakly positive and newly formed granules were most strongly stained with p38P antibodies (Fig. 1, B and C). The same pattern of codistribution was noted using either polyclonal or monoclonal antibodies (compare Fig. 1 with Fig. S1, A and B; available at http://www.jcb.org/cgi/content/full/jcb.200703174/DC1). Furthermore, cotransfection of fluorescent K18 and p38 resulted in colocalization of both proteins in prominent aggregates of living epithelial cells (Fig. S1, C and D). On the other hand, antibodies directed against the other phosphorylated MAPKs ERK and JNK did not react with OV-induced keratin granules (not depicted).

It is known that p38 phosphorylates specific keratin residues (Feng et al., 1999; Ku et al., 2002; Toivola et al., 2002). Using an antibody directed against keratin 8 (K8)-S73P, the major site in the K8 head domain that is phosphorylated by p38 (Liao et al., 1997; Ku et al., 2002), we could confirm previous results demonstrating that this epitope is virtually absent in normal-appearing interphase KF networks (Fig. 2, A–A″; Liao et al., 1997). Soon after OV addition, however, K8-S73P was readily detected on newly formed keratin granules (Fig. 2, B and C). In contrast, keratin phosphoepitope K8-S431P was present in both intact KF networks and keratin granules (Fig. S2, available at http://www.jcb.org/cgi/content/full/jcb.200703174/DC1). The same constitutive phosphorylation in untreated and OV-treated cells was also noted for K18-S33P (not depicted).

p38 activation promotes keratin granule formation and keratin phosphorylation

The consistently observed keratin aggregation in cells overexpressing p38-GFP (Fig. S1 C) suggested that p38 activation

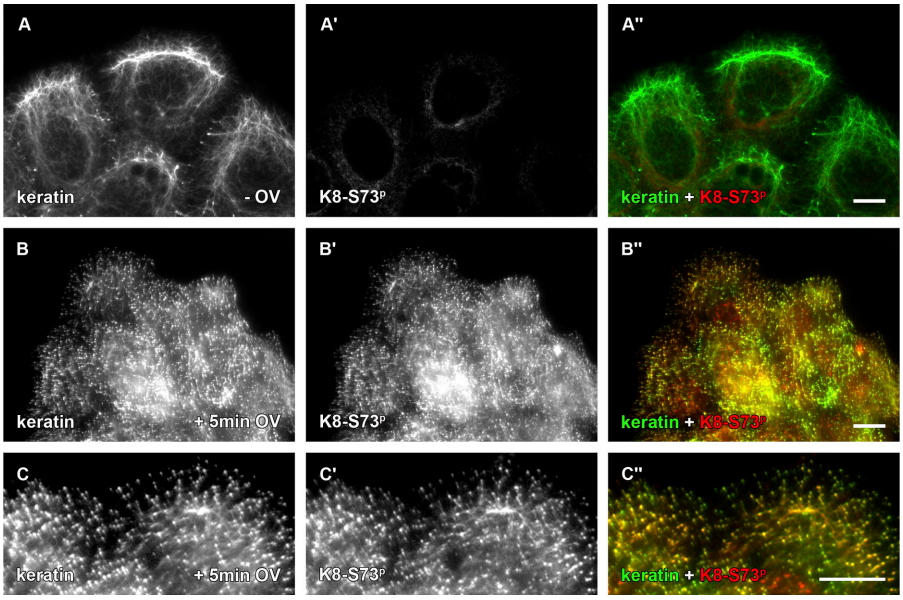

Figure 2. **K8 is rapidly and specifically phosphorylated on S73 upon p38P recruitment in OV-treated cells.** Fluorescence microscopy detecting HK13-EGFP in methanol/acetone-fixed AK13-1 cells (A–C) together with specific K8 epitope K8-S73P (A′–C′; merge in A″–C″) in untreated interphase cells (A–A″) and 5 min after addition of 20 mM OV (B–B″, C–C″). Note the appearance of K8-S73P epitopes in keratin granules. Bars, 10 μm.

determines keratin organization. To further examine this idea, A431 cells were transfected with the constitutively active p38 upstream regulators MKK3 and MKK6 (Raingeaud et al., 1996) either alone or in combination. These cells were identified by immunofluorescence microscopy detecting the attached Flag-tag (Fig. 3 A′), or by direct fluorescence microscopy of a linked CFP moiety (Fig. 3 B″). Transfected cells presented keratin granules that were positive for p38P (Fig. 3, B and B′) and contained K8-S73P epitopes (Fig. 3, C–C″). Many dead cells were noted 24 h after transfection, probably a consequence of p38-induced apoptosis, which was also noted in p38-GFP-producing cells. As an alternative to the slow-acting genetic p38 activation, pharmacological means were used to facilitate short-term induction and to prevent complex downstream effects of p38 action. Already 3 min after addition of the p38 activator anisomycin (Cano et al., 1996), abundant keratin granule formation was observed (see Fig. 3 D for 5-min time point) that was accompanied by p38P recruitment (Fig. 3, D′ and D″) and appearance of K8-S73P (not depicted). Collectively, these observations show that p38 activation leads to keratin reorganization and keratin modification.

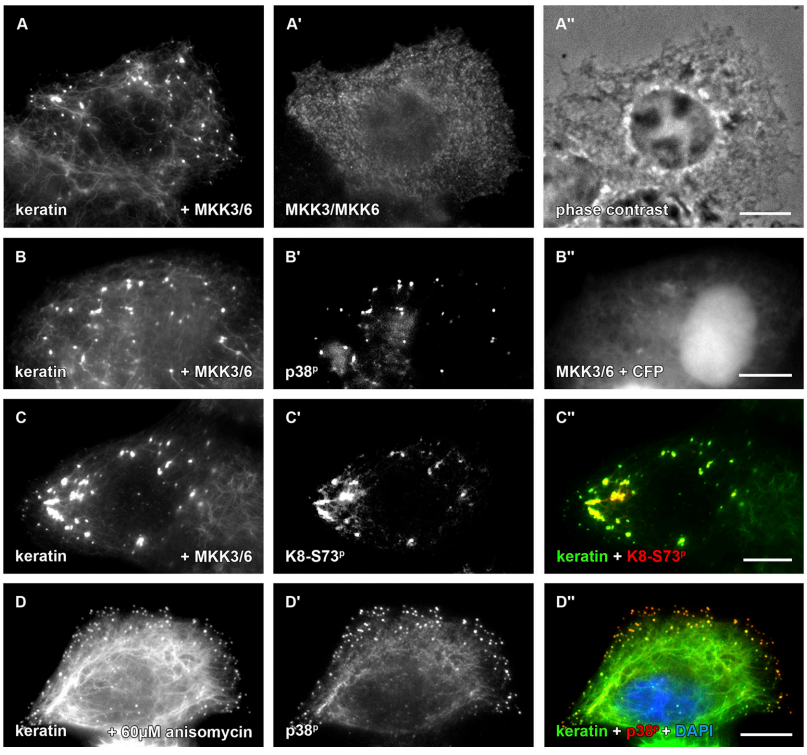

Figure 3. **Upstream p38 activators and pharmacological p38 inducers elicit keratin granule formation concomitant with recruitment of p38P to keratin granules and specific keratin phosphorylation.** Detection of HK13-EGFP fluorescence microscopy in formaldehyde-fixed (A and B) and methanol/acetone-fixed (C and D) AK13-1 cells either 24 h after double transfection with constitutively active MKK3 and MKK6 mutants (A–C) or after 5 min treatment with the p38 activator anisomycin (D; 60 μM). Transfected cells were identified either by antibody staining against the MKK3/6-associated Flag epitope (A′; corresponding phase contrast in A″) or by detection of the coexpressed CFP (B″). Note that the keratin granules form exclusively in the transfected cells and are positive for p38P (B′) and K8-S73P epitopes (C′). Similarly, anisomycin treatment resulted in formation of p38P-positive keratin granules (D′; merge in D″ together with DAPI staining). Bars, 10 μm.

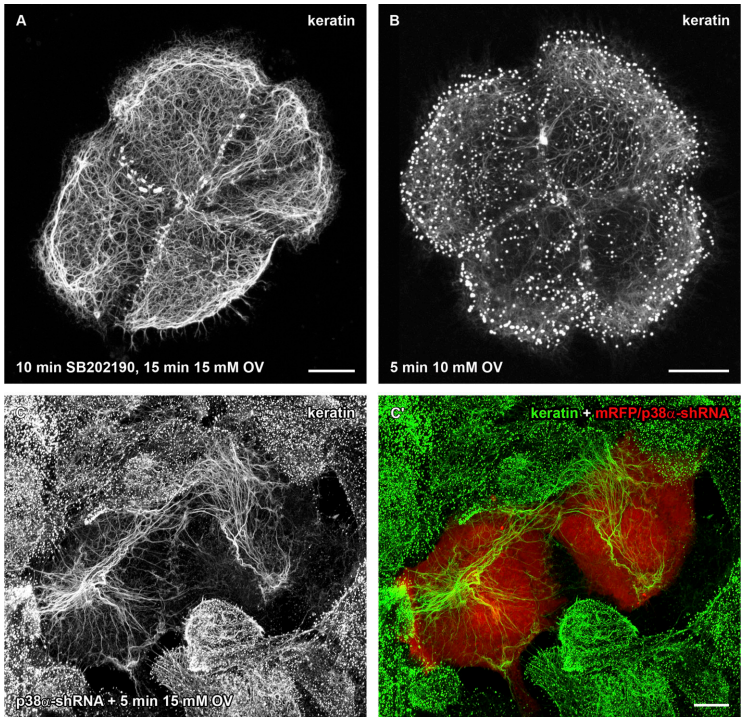

Figure 4. **Down-regulation of p38 activity prevents keratin granule formation in response to OV treatment.** p38 activity was either inhibited by treatment with 50 μM SB202190 for 10 min or by transfection with p38α-specific shRNA before incubation with OV for the indicated times. HK13-EGFP fluorescence was then assessed in the methanol/acetone-fixed AK13-1 cells by confocal laser scanning microscopy. Note that keratin granules are rapidly formed in cells without the p38 inhibitor (B) but not after pretreatment with SB202190 (A). Similarly, cells producing p38α-specific shRNA as identified by linked monomeric red fluorescent protein (mRFP) fluorescence (C′) present a keratin network that is not altered by OV (C and C′). Bars, 10 μm.

p38 inactivation prevents keratin granule formation

Conversely, A431 cells were treated with specific p38 inhibitors. In addition to the previously used p38 inhibitor SB203580 (Strnad et al., 2003), we tested SB202190 that also preferentially interferes with the α and β isoforms of p38 (Davies et al., 2000). This treatment did not disrupt the KF network over a wide concentration range, although KFs appeared to coalesce and concentrate gradually in the central cytoplasm over time. When, in addition, cells were incubated with OV, keratin granule formation was efficiently prevented (compare Fig. 4 A with Fig. 4 B). To down-regulate p38 synthesis genetically, expression of p38 isoforms was first determined by RT-PCR. α, γ, and δ isoforms could be amplified from AK13-1 cells but not p38-β. Therefore, plasmids were constructed encoding α-, δ-, and δ/γ-specific p38 shRNAs together with fluorescent indicator proteins. Transfected AK13-1 cells exhibited considerable reorganization of the keratin cytoskeleton in each instance (Fig. S3, A and B; available at http://www.jcb.org/cgi/content/full/jcb.200703174/DC1). A substantial depletion of KFs was seen in most parts of the cytoplasm, sparing only desmosome-anchored filaments. Most material coalesced in a juxtanuclear position. It still contained filaments that were compacted, but did not aggregate into granules. When these cells were treated with OV, the remaining filaments did not form granules as in neighboring nontransfected cells (Fig. 4, C and C′).

Collectively, the data suggested that the p38 K8-S73 target residue contributes to keratin granule formation. We therefore decided to compare the KF network-forming properties of the phosphorylation-incompetent K8-S73A mutant and the K8-S73D mutant mimicking constitutive phosphorylation. When introduced together with human K18 chimera HK18-YFP into A431 cells, only 31.33 ± 3.87% of K8-S73A–producing cells contained keratin granules (n = 560; four experiments) whereas 59.9 ± 1.59 of K8-S73D–producing cells presented abundant granules (n = 604; four experiments). To abolish the mitigating effects of endogenous wild-type keratins, K8 constructs were transfected together with HK18-YFP chimeras into SW13 cells that lack cytoplasmic IFs (compare Wöll et al., 2005). In each instance, however, a normal-appearing KF network was formed (for similar results in NIH-3T3 cells, see also Ku et al., 2002), although an increase in the soluble pool of cells producing K8-S73D cannot be excluded (Fig. S3, C and D). Turnover of these K8 mutant-containing networks and motility of KF precursors were analyzed by time-lapse fluorescence microscopy and FRAP. No differences were noted in comparison to cells producing only wild-type keratins (unpublished data). In addition, motility of cells transfected with mutant K8 constructs was indistinguishable from cells synthesizing wild-type keratins. These results demonstrate that K8-S73^{p} alone is not sufficient to mediate KF network rearrangements, although it appears to contribute, in combination with other factors, to keratin rearrangement in a cell context–dependent fashion.

Keratin granule formation coincides with a rapid increase in p38 and K8-S73 phosphorylation

To examine the extent of phosphorylation of p38 and keratins upon keratin granule formation, biochemical analyses were performed of cells treated with OV. A rapid and considerable rise of p38^{p} was readily detectable in immunoblots of total cell lysates in response to OV (Fig. 5 A). Furthermore, reaction of cytoskeletal fractions with antibodies directed against K8-73^{p} revealed a similarly rapid and coincident increase (Fig. 5 B), whereas no changes were observed for other keratin phosphoepitopes (Fig. 5 C). To examine interactions between keratins and p38,

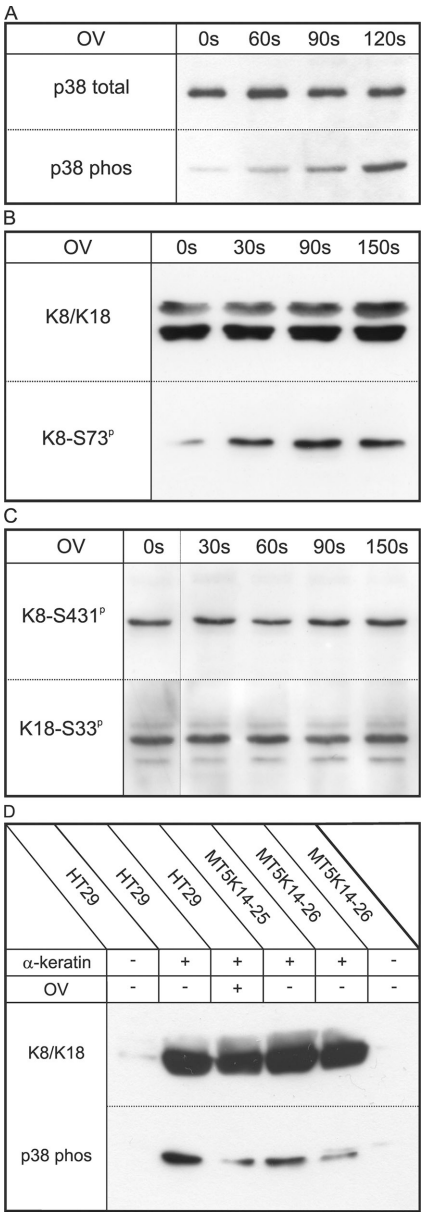

Figure 5. **OV treatment leads to rapid increase of p38 and K8-S73 phosphorylation.** Immunoblots of total cell lysates (A) and cytoskeletal extracts (B and C) that were prepared from AK13-1 cells detecting all p38 polypeptides (p38 total), phosphorylated p38 (p38 phosp), all keratin 8/18 polypeptides (K8/K18), K8 phosphoepitopes S73^{P} (K8-S73^{P}) and S431^{P} (K8-S431^{P}), and keratin 18 phosphoepitope S33^{P} (K18-S33^{P}). Cells were treated with 20 mM OV for up to 150 s in the dark. Polypeptides were separated by 10% SDS-PAGE and transferred onto nitrocellulose membranes before incubation with primary and HRP-coupled secondary antibodies. Bound antibodies were detected with the help of the ECL system. The bottom and top blots in A were obtained from gels containing the same samples that were run in parallel; the bottom blots in B and C were obtained after stripping of the top blots of each, respectively. Note the rapid and specific increase of p38^{P} and K8-S73^{P} in OV-treated cells. (D) Immunoblot of immunoprecipitates that were prepared with the help of antibodies L2A1 directed against keratin 8/18 polypeptides from colon carcinoma-derived HT29 cells and mammary adenocarcinoma-derived MCF7 subclones MT5K14-25 producing EYFP-K14 and MT5K14-26 producing mutant EYFP-K14$_{R125C}$. The fluorogram depicts the reaction of antibodies directed either against keratins 8/18 and p38^{P} as detected with the ECL system in the immunoprecipitates that had been separated by nondenaturing 10% SDS PAGE and blotted onto nitrocellulose. Note that preincubation of HT29 cells with 20 mM OV for 4 min did not increase the amount of coprecipitated p38^{P} and that p38^{P} did not preferentially associate with precipitable mutant keratins.

coimmunoprecipitation experiments were performed. Using different detergents including NP-40 and empigen BB (Lowthert et al., 1995), we were able to detect p38^{P} in anti-keratin precipitates from colon carcinoma-derived HT29 cells whose level was, however, not increased upon OV treatment in these cells or in AK13-1 cells (Fig. 5 D; unpublished data). Either we were not able to solubilize the newly formed keratin granules efficiently (see also Windoffer and Leube, 2001), and/or existing bonds were disrupted during cell fractionation.

Phosphorylated keratin granules that are generated in various stress situations colocalize with p38^{P}

To investigate whether p38^{P} recruitment and simultaneous increase of site-specific keratin phosphorylation apply also to other situations when keratin granules are formed, AK13-1 cells were subjected to various types of stress. A 5-min incubation at 60°C induced keratin granules that were most prominent in peripheral regions and colocalized with p38^{P} (Fig. 6 A). Hypotonic stress that was applied by incubation in 150 mM urea resulted in reorganization of the KF system into clumped material that also stained for p38^{P} (Fig. 6 B). Conversely, hypertonic stress also induced disassembly of the KF network into granular material. p38^{P} antibodies reacted again specifically with the granular material, but not with the remaining thin filaments (Fig. 6, C and D). The K8-S73^{P} epitope was also detected in the granular material in each situation (not depicted). These observations support the notion that p38 recruitment is a general mechanism that is associated with KF phosphorylation and reorganization.

KF network alterations occurring during the cell cycle coincide with p38^{P} recruitment and keratin phosphorylation

Considerable keratin reorganization takes place during mitosis, and it was reported that A431-cells almost completely disassemble their network into soluble material and rapidly moving keratin granules during early prophase (Windoffer and Leube, 1999, 2001). When we stained dividing AK13-1 cells with p38^{P} antibodies, an almost complete colocalization with forming keratin granules was noted during metaphase (Fig. 7, B–B″). In very early prophase, KFs disintegrated into p38^{P}-positive granules (Fig. 7, A–A″). Occasionally, cells were seen with intermediate phenotypes, i.e., with dense filament bundles or granules emanating from thin filaments, both of which may correspond to intermediate stages of either assembly or disassembly (Fig. 7, C–C″). Interestingly, peripheral parts of KF networks were sometimes labeled by p38^{P} antibodies in areas of cells that did not attach directly to neighboring cells but contained lamellipodial-like extensions (not depicted). These areas were recently identified as regions of high KF turnover (Wöll et al., 2005; Windoffer et al., 2006). K8-S73^{P} appearance was noted in each instance (not depicted).

Mutant keratin granules colocalize with p38^{P} and K8-S73^{P}

Given that p38^{P} is recruited to keratin granules that are formed in very different situations, we decided to examine the composition

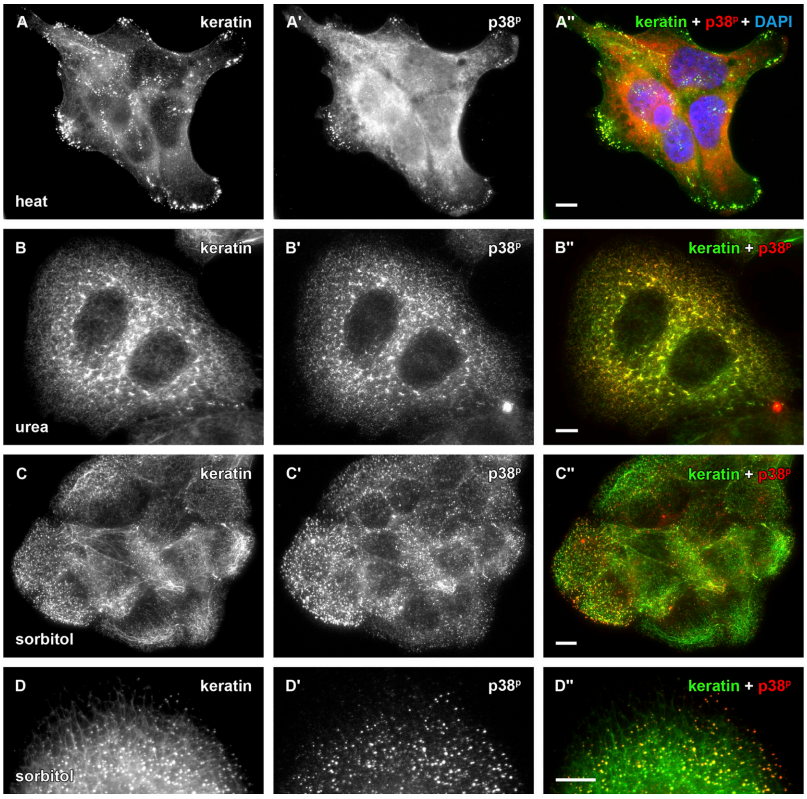

Figure 6. **p38ᵖ codistributes with keratin granules in various stress situations.** Detection of keratin (HK13-EGFP fluorescence; A–D) and p38ᵖ distribution (immunofluorescence in A′–D′; merged images in A″–D″) in methanol/acetone-fixed AK13-1 cells subjected to different types of stress. Cells were either subjected to a 5-min heat stress at 60°C (A–A″), incubated for 7 min in 150 mM urea (B–B″), or treated for 10 min with 200 mM sorbitol (C–C″; higher magnifications in D–D″). Note that newly formed keratin granules colocalize specifically with p38ᵖ in each instance. Bars, 10 μm.

of granules containing mutant keratins. We used MCF7-derived cell line MT5K14-26, producing mutant EYFP-K14$_{R125C}$ fluorescent chimeras (Werner et al., 2004). The abundant peripheral keratin granules were strongly stained by p38ᵖ antibodies, whereas the residual perinuclear KFs were not (Fig. 8, B–B″). In comparison, cell line MT5K14-25 synthesizing wild-type fluorescent K14 chimera EYFP-K14 presented only diffuse p38ᵖ fluorescence (Fig. 8, A–A″). Coimmunoprecipitation experiments, however, did not reveal an increased association of keratins with p38ᵖ in the mutant cells, possibly due to the inability to solubilize the p38ᵖ-positive granular material or due to disruption of the association during immunoprecipitate preparation (Fig. 5 D). Quantification of the p38 level in MT5K14-25 and MT5K14-26 showed that total p38 was the same in both, whereas p38ᵖ was twofold increased in EYFP-K14$_{R125C}$ cells (Fig. 8, C–E), reminiscent of the reported increase of JNKs in keratinocytes expressing other keratin mutants (D'Alessandro et al., 2002). Furthermore, endogenous keratins colocalized with the mutant polypeptides and K8-S73ᵖ epitopes were seen in perinuclear filaments and most prominently in keratin granules (Fig. 9, C–C″). In contrast, this epitope was only expressed in mitotic cells of line MT5K14-25 (Fig. 9, A–A″). Similar to A431-derived cells, all different keratin organizational forms were positive for K8-S431ᵖ in both MCF7-derived cell lines (Fig. 9, B and D).

p38 inhibitors interfere with KF precursor formation and mutant keratin granule disassembly

Fig. 4 shows that p38 inhibitors do not result in immediate KF network disassembly, although long-term down-regulation resulted in network depletion (Fig. S3). To find out whether dynamic aspects of KF organization are altered in these conditions, time-lapse fluorescence microscopy was performed. A typical sequence is shown in Fig. 10 A and Video 1 (available at http://www.jcb.org/cgi/content/full/jcb.200703174/DC1). Addition of the p38 inhibitor SB202190 led to an increased concentration of the fluorescent KF network toward the central cytoplasm. This altered arrangement was, however, not caused by cell retraction because the periphery remained in place and continued to exhibit high ruffling activity with multiple dynamic filopodial extensions. Remarkably, the peripheral cytoplasmic area did not contain KF precursors that are usually generated in this region (Windoffer et al., 2004). Stress fibers were noted in close proximity to the periphery of the retracted keratin network (Fig. 10 A′, arrowheads).

To find out whether a similar inhibition of KF precursor formation occurs also in cells producing mutant keratins, MT5K14-26 cells were treated with SB202190 (Fig. 10 B and Video 2; available at http://www.jcb.org/cgi/content/full/jcb.200703174/DC1). KF precursor formation ceased immediately after drug application. At the same time, ruffling activity of the peripheral cytoplasm continued. Upon washout of the drug, keratin particle formation resumed in the peripheral cytoplasm. Despite these strong effects of p38 inhibition on keratin particle formation, cells retained keratin granules even after extended periods of SB202190 treatment (unpublished data). Time-lapse fluorescence analysis helped to solve this apparent paradox, revealing that keratin particles became stabilized upon p38 inhibition (Videos 2 and 3). The rapid dissolution observed in untreated MT5K14-26 cells (see also Werner et al., 2004) was almost

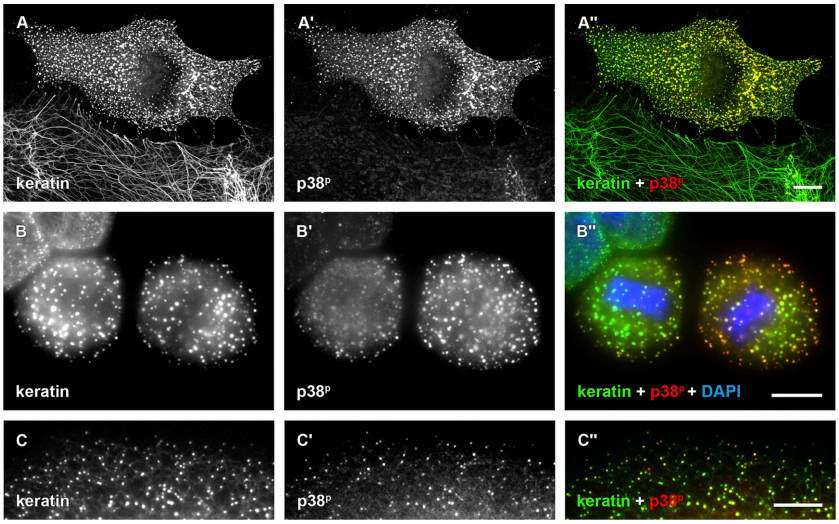

Figure 7. **p38ᴾ associates transiently with keratins during mitosis.** The fluorescence images (laser scanning microscopy in A–A″; epifluorescence microscopy in B–C″) show the distribution of HK13-EGFP and p38ᴾ in methanol/acetone-fixed AK13-1 cells during different stages of mitosis. Note the specific codistribution of keratin granules with p38ᴾ. Bars, 10 μm.

completely abolished. In sum, our observations highlight the importance of p38 activity for KF precursor formation and KF network turnover.

Discussion

The current study identified p38 as a major regulator of KF network formation by revealing a tight temporal and spatial correlation between activation of p38, recruitment of p38ᴾ to KFs, keratin phosphorylation at specific p38 target sites, and ensuing disassembly of KFs into granules. This sequence of events was observed during physiological situations of KF reorganization, most notably in dividing cells, in cells subjected to stress and, quite remarkably, in cells producing mutant keratins (summary of colocalization results in Fig. S4, available at http://www.jcb.org/cgi/content/full/jcb.200703174/DC1). Furthermore, experimental up-regulation of p38 activity led to keratin granule formation, whereas its down-regulation prevented it. The speed and reversibility of the observed p38-dependent processes make them highly suitable to accomplish transient network attenuations

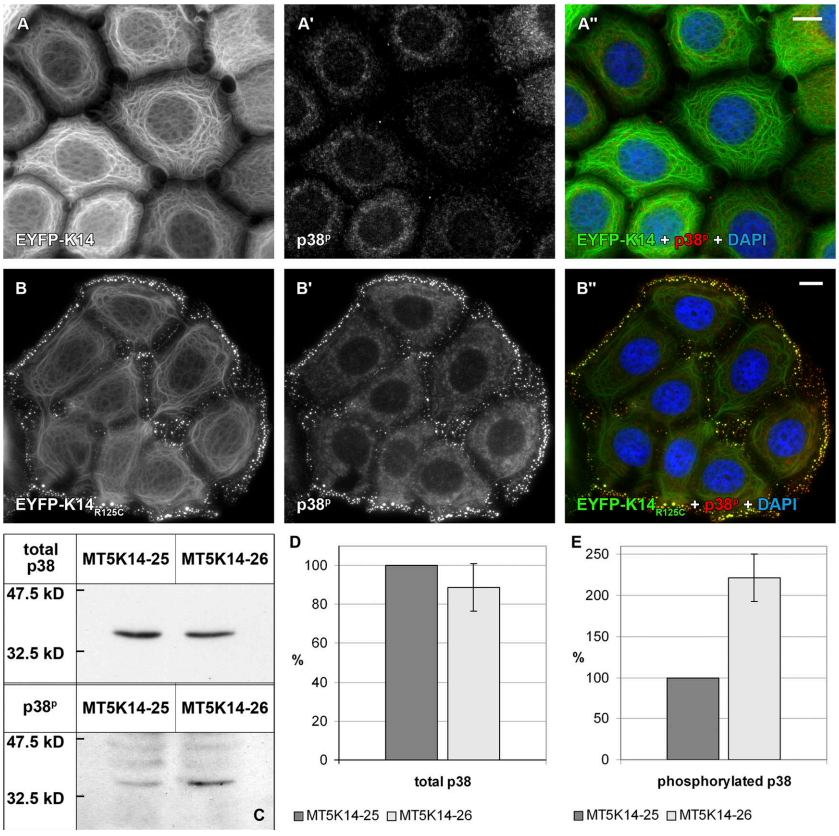

Figure 8. **p38ᴾ colocalizes specifically with mutant keratin granules and is increased in cells producing mutant keratins.** (A and B) Fluorescence images show methanol/acetone-fixed MCF7 cells stably transfected with fluorescent keratin 14 chimera EYFP-K14 (A; cell line MT5K14-25) or mutant keratin 14 chimera EYFP-$K14_{R125C}$ (B; cell line MT5K14-26) and stained with anti-p38ᴾ antibodies (A′ and B′; merged images in A″ and B″ together with DAPI staining). Note the selective codistribution of mutant keratin granules with p38ᴾ. Bars, 10 μm. (C–E) Detection of total p38 and p38ᴾ in total cell lysates of MT5K14-25 and MT5K14-26 cells by immunoblotting (C). The positions and molecular weights of co-electrophoresed size markers are shown. (D and E) histograms summarizing quantitative immunoblotting results ($n = 4$) obtained from determinations of the integrated optic densities of bands in fluorograms revealing total p38 and p38ᴾ. The values determined in MT5K14-25 cells were defined as 100%. Note that in MT5K14-26 cells the level of total p38 is not significantly different (90 ± 6.8%; $P = 0.343$), but that p38ᴾ is considerably increased in these cells (220 ± 29.9%; $P \leq 0.001$).

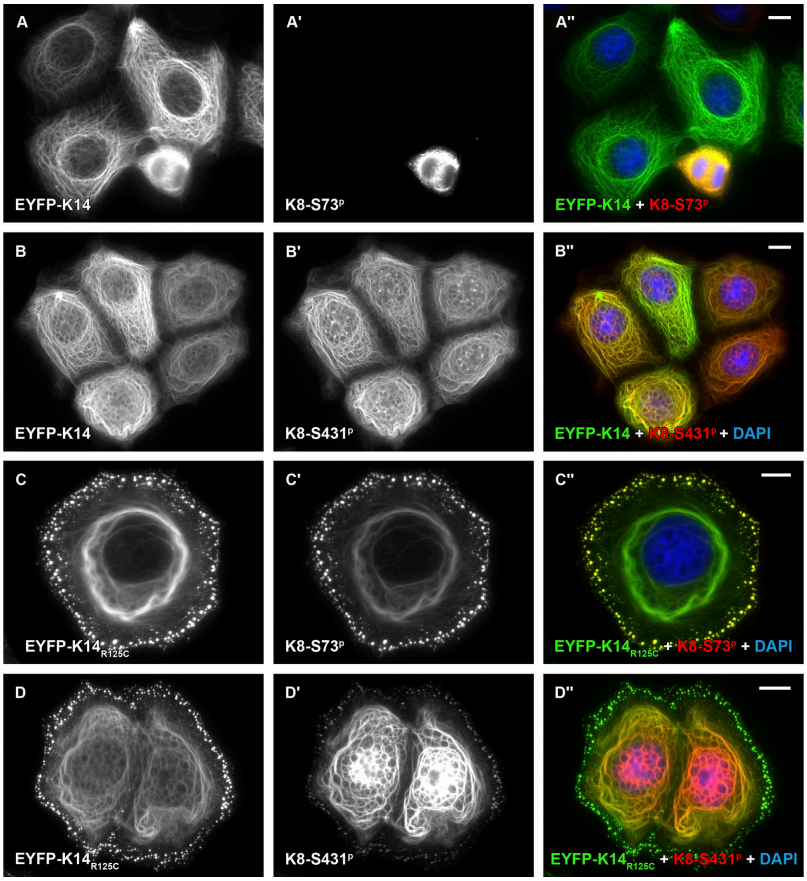

Figure 9. **Wild-type K8 is specifically phosphorylated on S73 in mitotic keratin aggregates and in keratin granules containing mutant keratins.** Fluorescence microscopy of methanol/acetone-fixed MCF7 cell lines producing fluorescent keratin 14 chimera EYFP-K14 (A and B; line MT5K14-25) or mutant keratin 14 chimera EYFP-K14$_{R125C}$ (C and D; line MT5K14-26). Note the restricted codistribution of mitotic keratins and mutant keratin granules/KF bundles with K8-S73^{P} (A′ and A″; C′ and C″) in contrast to the constitutive colocalization of the K8-S431^{P} epitope with all keratin forms (B′ and B″; D′ and D″). Bars, 10 μm.

in various in vivo situations that require finely tuned cell shape changes. Indeed, p38 is present in epithelial cells and responds rapidly (i.e., within a few minutes) to various types of stress. These include physiologically relevant mechanical pressure (Hofmann et al., 2004), osmotic shock (Garmyn et al., 2001; Cheng et al., 2002), and UV irradiation (Chen and Bowden, 1999). Moreover, p38 is induced in keratinocytes upon wounding (Harper et al., 2005). Accordingly, it has been observed that keratinocyte outgrowth from human skin explants and keratinocyte migration are dependent on p38 (Klekotka et al., 2001; Bakin et al., 2002; Sharma et al., 2003; Stoll et al., 2003). Furthermore, p38 is activated by proinflammatory cytokines in A431 cells (Wery-Zennaro et al., 2000) and is increased in psoriatic skin (Johansen et al., 2005). The migrating and dynamic keratinocytes require increased flexibility of their cytoskeleton that may in part be provided by p38-mediated keratin network alterations. In support, p38^{P} staining was frequently observed in lamellipodia in our cell systems. The relevance of p38 activity in epithelial physiology is further underscored by the recent observation that pemphigus vulgaris IgGs that bind to the extracellular portion of the desmosomal cadherin desmoglein 3 induce "retraction" of the KF system via p38 (Berkowitz et al., 2005). Collectively, overwhelming evidence exists demonstrating a prominent role of p38 in short-term regulation of epithelial plasticity that should be distinguished from long-term effects on keratinocyte differentiation and apoptosis (Eckert et al., 2002, 2003; Efimova et al., 2003). Furthermore, functions of p38 signaling are apparently not restricted to keratins, but are also of relevance for vimentin (Cheng and Lai, 1998) and neurofilaments (Ackerley et al., 2004). On the other hand, other stress-activated protein kinases may be involved in IF organization, although activated JNKs and ERKs were not found in association with keratin granules in our cell systems. Yet, in other cells, K8 has been identified as a binding partner of JNKs that also phorphorylate K8-S73 in vitro (He et al., 2002) and are elevated in cells producing mutant keratins (D'Alessandro et al., 2002). Similarly, altered phosphorylation, presumably mediated by ERK1/2, has been reported for K8-S431 upon EGF stimulation and in response to osmotic stress (Ku and Omary, 1997; Tao et al., 2006).

Our results in combination with many other publications (compare Inagaki et al., 1996; Izawa and Inagaki, 2006; Omary et al., 2006) strongly suggest that keratin phosphorylation is the primary mechanism by which the keratin network is reorganized. K8-S73 has received particular attention because it presents an on/off behavior during mitosis, in various stress situations including shear stress, and during apoptosis (Liao et al., 1997; Feng et al., 1999; Ridge et al., 2005). Furthermore, the sequence motif surrounding K8-S73 is conserved among several type II keratins as LLS/TPL where the corresponding threonine residue is also phosphorylated by p38 in an on/off fashion, leading to increased keratin solubilization, filament reorganization, and collapse during mitosis and UV- or anisomycin-induced apoptosis, as well as in psoriatic skin and squamous cell carcinoma (Toivola et al., 2002). Phosphorylation of sites in the head domain has been shown to be essential for the assembly

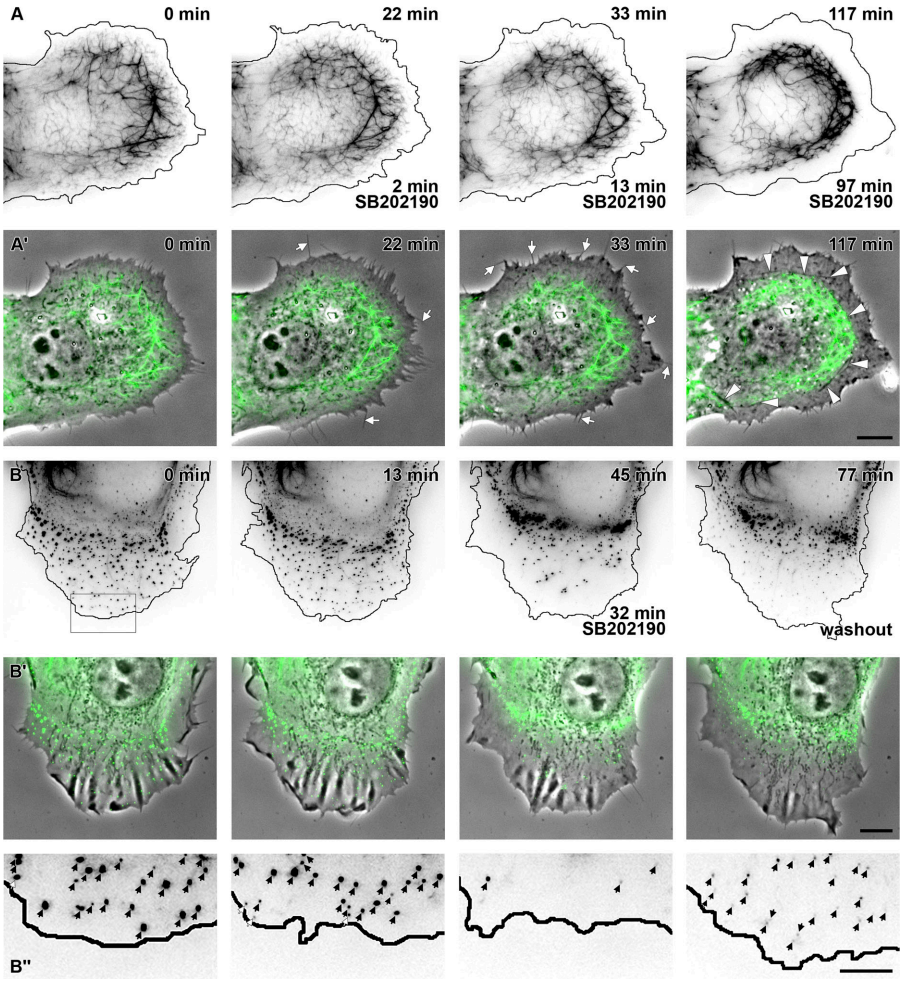

Figure 10. **Inhibition of p38 activity prevents KF precursor formation and dissolution of mutant keratin granules.** Image series (presented as inverse fluorescence micrographs) were taken from time-lapse recordings, Video 1 depicting HK13-EGFP dynamics in AK13-1 cells (A and A′) and Video 2 showing EYFP-K14$_{R125C}$ fluorescence in MT5K14-26 cells (B–B″) and corresponding phase contrasts (overlays in A′ and B′). Cells were treated with the p38 inhibitor SB202190 (100 μM) as indicated. The positions of the plasma membranes as determined from phase-contrast images are demarcated in A, B, and B″. Note the retraction of the wild-type KF network in response to the drug while filopodia are still abundant (A′, arrows) and the presence of prominent stress fibers (arrowheads) adjacent to the outermost KFs. The image series in B demonstrates the transient cessation of keratin granule formation and simultaneous granule stabilization (see also Video 3) upon drug administration (see also high magnification of boxed area in B″ with arrows on newly formed KF precursors). Bars: (A, A′, B, and B′) 10 μm; (B″) 5 μm.

of different IF types (Inagaki et al., 1990; Gibb et al., 1996; Gohara et al., 2001; Herrmann et al., 2003; Kreplak et al., 2004). The increase in negative charge by phosphorylation is believed to prevent interactions of the head domain with the negatively charged rod thereby keeping the head in an "open" configuration. Presumably, this configuration is part of opening up the filament structure during disassembly into granules and may also be needed during intermediate assembly steps. The observed p38-dependent and head domain–specific phosphorylation of K8-S73 before KF disassembly, as well as the inhibition of both KF precursor formation and mutant keratin granule disassembly by the p38 inhibitor SB202190, strongly support this notion (Videos 1–3). Yet, further experiments are needed to find out whether network disintegration into granules is due to keratin disassembly or simply a "clumping" of filaments, both of which may be determined by phosphorylation. Further support for the importance of head domain phosphorylation was provided for vimentin, in which case S55A mutants were shown to prevent network disassembly during mitosis (Chou et al., 1996). Similarly, light chain neurofilament S55D mutants interfered with proper neurofilament assembly in cultured cells and transgenic mice (Gibb et al., 1996, 1998). On the other hand, K8-S73^{p} is not alone sufficient for KF network disruption (Fig. S3; Ku et al., 2002), indicating that additional p38 target sites in K8 and/or other keratins are necessary. Constitutive differences in overall keratin phosphorylation could well explain the different reactivities of KF networks in different cell types during mitosis and in various stress situations (compare Windoffer and Leube, 1999), and, even more, the observed lack of keratin reorganization in vivo, e.g., in K8-S73^{p}-containing hepatocytes (Toivola et al., 2004). It has been proposed, therefore, that multiple events of phosphorylation and dephosphorylation cooperate in KF organization (Tao et al., 2006). Cooperation of several phosphorylation sites for IF formation has also been documented for GFAP in transgenic mice (Takemura et al., 2002), and the importance of cross talk between head and tail domain phosphorylation for neurofilament assembly in specific cellular topologies has been described (Zheng et al., 2003). Finally, we cannot exclude that p38 activity affects, in addition to keratins, factors which in turn regulate KF properties (Liao and Omary, 1996; Ku et al., 2004; Tao et al., 2005).

The strong and highly specific staining of cytoplasmic granules containing mutant keratins with antibodies against p38^{p} and K8-S73^{p} was not expected, and we were even more surprised to be able to almost instantaneously prevent keratin granule formation by pharmacological p38 inhibition. Interestingly, hyperphosphorylated keratin granules are present in toxic liver disease in the form of cytoplasmic Mallory bodies

(Stumptner et al., 2000; Fickert et al., 2003; Toivola et al., 2004; Zatloukal et al., 2004), whose formation also relies on p38 activity (Nan et al., 2006). p38 activity is likely also relevant for other IF aggregates that occur in many different diseases, including cardiac myopathy, glial Alexander disease, and several neurodegenerative diseases (Al-Chalabi and Miller, 2003; Helfand et al., 2003; Omary et al., 2004). Notably, neurofilament aggregates that are formed in motoneurons of patients suffering from amyotrophic lateral sclerosis contain $p38^P$ together with phosphorylated NF-M and NF-H (Ackerley et al., 2004; Bendotti et al., 2004). A similar colocalization was also noted in a transgenic mouse model of amyotrophic lateral sclerosis (Tortarolo et al., 2003; Bendotti et al., 2004). In addition, mimicking-increased IF phosphorylation by expression of the NF-L S55D mutants led to prominent neuropathology with neurofilament inclusion bodies in neuronal perikarya and swollen axons in transgenic mice (Gibb et al., 1998).

While this investigation focused on the consequences of p38 recruitment for structural and dynamic properties of the keratin cytoskeleton, several publications have provided evidence that this interaction bears also important consequences for cell physiology. In particular, it has been suggested that keratins act as a phosphate "sponge" for stress-activated kinases based on observations in transgenic mice overexpressing K8-S73A and presenting increased susceptibility to liver injury and apoptosis (Ku and Omary, 2006). Our data, however, extend this model by demonstrating that activated p38 is not simply bound to the IF cytoskeleton, but also induces considerable organizational alterations and thereby affects cell shape, flexibility, and most likely other basic cellular functions (Kim et al., 2006).

Materials and methods

DNA cloning

cDNAs coding for HK8-CFP and HK18-YFP have been described previously (Strnad et al., 2002; Wöll et al., 2005), and a cDNA for HK18-RFP was obtained from Anne Kölsch (this institute). A cDNA in the EcoRI site of Bluescript coding for keratin mutant K8-S73A was provided by Dr. Omary (Stanford University, Palo Alto, CA; Ku et al., 2002). The ~600- bp HindIII fragment encompassing the mutated part of K8 was excised and exchanged for the corresponding wild-type fragment in HK8-ECFP–encoding plasmid that was described recently (Windoffer et al., 2004). In addition, a cDNA coding for K8-S73D mutant in a mammalian expression vector was also given to us by Dr. Omary (Ku et al., 2002).

A p38-GFP cDNA was given to us by Dr. Bradham (Duke University, Durham, NC; Bradham and McClay, 2006). Flag-tagged cDNAs coding for constitutively active MKK3 (in pRc/RSV) and MKK6 (in pCDNA3) were provided by Dr. Davis (University of Massachusetts Medical School, Worcester, MA; Raingeaud et al., 1996). The HindIII/SpeI fragment coding for MKK3 was further subcloned into the corresponding sites of modified plasmid pTER (van de Wetering et al., 2003) containing additional CMV promoter-driven fragments coding for either ECFP (pTER-ECFP) or mRFP (pTER-mRFP; see Windoffer et al., 2006). In the case of MKK6, the MKK6-encoding plasmid and both pTER derivatives were cleaved with XbaI, blunt-ended, and cut with HindIII before ligation.

To specifically knock down p38 isoforms, shRNA-producing constructs were prepared. To this end, oligonucleotides encoding shRNAs were inserted into the BglII/HindIII sites of either pTER-ECFP or pTER-mRFP. For annealing, 10 pM of complementary oligonucleotides were incubated in annealing buffer (100 mM potassium acetate, 30 mM Hepes-KOH, pH 7.4, and 2 mM magnesium acetate) for 5 min at 95°C, 10 min at 70°C, and cooled down to room temperature. Subsequently, they were either stored at −20°C or used directly for ligation with plasmid DNA. Oligonucleotide pairs α1-sense/α1-antisense and α2-sense/α2-antisense were used to deplete p38α RNA, oligonucleotide pairs δ2-sense/δ2-antisense and δ3-sense/δ3-antisense to degrade p38δ, and oligonucleotides δ1/γ1-sense/δ1/γ1-antisense to target p38α and δ (Fig. S5).

RT-PCR

RT-PCR using the Enhanced Avian Reverse Transcriptase kit (Sigma- Aldrich) was performed for amplification of RNAs coding for specific p38 isoforms. The oligonucleotides used to amplify the α, β, γ, and δ isoforms are listed in Fig. S5.

Cell culture

The following cell lines were propagated as described previously: vulva carcinoma-derived A431 cells of clones E_3 and AK13-1 (Windoffer and Leube, 1999), colon adenocarcinoma-derived HT29 cells (ATCC HTB 38), spontaneously immortalized mammary epithelial EpH4 cells (compare Windoffer et al., 2006), and mammary adenocarcinoma-derived MCF7 cells of lines MT5K14-25 producing EYFP-K14 and MT5K14-26 synthesizing EYFP-$K14_{R125C}$ (Werner et al., 2004). Foreign DNA was transfected into subconfluent cells by using the Lipofectamine 2000 reagent following the instructions provided by the manufacturer (Invitrogen; Windoffer and Leube, 2004).

OV was obtained from Sigma-Aldrich and a 1M stock solution was prepared in ddH_2O. The dissolved drug was added to subconfluent cultured cells in the dark at final concentrations between 10 and 30 mM for 5–10 min. To specifically inhibit p38α and β activity, cells were treated with SB202190 (Sigma-Aldrich) at final concentrations ranging from 50 to 100 μM. To induce p38 activity pharmacologically, cells were incubated with anisomycin (Sigma-Aldrich) at 30 μM. In hyperosmotic stress assays, cells at 70–80% confluence were incubated in medium containing 200 mM sorbitol for 5–25 min at 37°C before fixation. Hypoosmotic stress conditions were attained by incubation in medium supplemented with 150 mM urea for 5–15 min at 37°C. Cells recovered subsequently in normal medium for 5–20 min before further processing. For heat stress, subconfluent cells were placed in a 60°C incubator for 5–10 min and were then fixed.

Fluorescence microscopy and antibodies

In most instances cells were fixed by incubation for 5 min in −20°C cold methanol followed by a short 10-s treatment with −20° cold acetone. After air drying, cells were ready for antibody incubation. To detect soluble fluorescent proteins it was necessary to fix cells for 10 min at 4°C in 3% formaldehyde freshly prepared in PBS. A short 1-min treatment with 0.01% digitonin in PBS followed at room temperature. Alternatively, cells were treated with −20°C cold methanol for 10 min. After a subsequent 10-min incubation in 4°C PBS, cells were treated with 5% bovine serum albumin for 15 min at room temperature. Further antibody incubations followed in the same way as for methanol/acetone-fixed cells (Windoffer and Leube, 2004).

The following antibodies were used: polyclonal rabbit antibodies directed against total p38, dual phosphorylated p38 (recognizing $T180^P$/$Y182^P$), total JNK, JNK^P, total ERK1/2, $ERK1/2^P$, and against the Flag epitope DYDDDK were obtained from New England Biolabs, Inc.; murine monoclonal antibodies against dual phosphorylated p38 (recognizing $T180^P$/$Y182^P$) were from New England Biolabs Inc.; and monoclonal antibodies against $K8\text{-}S73^P$ (LJ4), $K8\text{-}S431^P$ (5B3), $K18\text{-}S33^P$ (IB4), and total K8/K18 (L2A1) were provided by Dr. Omary (Ku and Omary, 1997; Liao et al., 1997); secondary antibodies were ordered from Dianova and Rockland. Images were recorded with an inverse fluorescence microscope (IX-70; Olympus) and an attached slow scan camera (model IMAGO, Till Photonics; Windoffer and Leube, 2004; Windoffer et al., 2006). In some instances a confocal laser scanning microscope was used (SP5; Leica). Pictures were edited with Adobe Photoshop CS software to prepare figures.

Pearson coefficients were determined to quantify colocalization of different fluorescence patterns using Image-Pro Plus software (Media Cybernetics).

Live-cell imaging

Recording of phase-contrast images and fluorescence patterns on an inverse fluorescence microscope were performed as described previously (Windoffer and Leube, 2004; Windoffer et al., 2006).

Cell fractionation and immunoblotting

Total cell lysates were prepared by adding 200–500 μl buffer (62.5 mM Tris-HCl, 2% [wt/vol] SDS, 10% glycerol, 50 mM DTT, and 0.01% [wt/vol] bromophenol blue) per 100 mm Petri dish. Solubilized cells were scraped off, sonicated briefly, and heated to 95°C for 5 min before SDS-PAGE.

Cytoskeletal fractions were prepared by standard procedure (compare Windoffer and Leube, 2004). SDS-PAGE and immunoblotting was done as described previously (Strnad et al., 2002). In some instances, membranes were stripped by incubation in buffer containing 62.5 mM Tris, 2% (wt/vol) SDS, and 100 mM mercaptoethanol for 30 min at 55°C.

Immunoreactions were quantified by scanning fluorograms and analyzing reactive bands with Gel-Pro Analyzer software (Bio-Rad Laboratories). Integrated optic densities were determined from immunoblots run in parallel examining cell fractions from different experiments. The mean, SEM, and P values were calculated with SigmaStat (SYSTAT Software, Inc.).

For immunoprecipitation, cells were washed twice with PBS supplemented with 5 mM EDTA, scraped off, and solubilized in ice-cold buffer containing 1% NP-40, 5 mM EDTA, and 0.1 mM PMSF together with protease inhibitors (1 tablet of protease inhibitor cocktail "cOmplete" from Roche per 50 ml) by incubation at 4°C in a shaker for 2 h. Particles were centrifuged down at 18,000 *g* for 20 min at 4°C. Keratin antibody L2A1 was added to the supernatant. After incubation for 1 h, preequilibrated protein A–Sepharose CL-4B (GE Healthcare) was added and incubation at 4°C continued for another 2 h under constant agitation. Three brief wash steps in buffer containing 0.1% NP-40, 5 mM EDTA, and 0.1 mM PMSF followed and the remaining material was suspended in 62.5 mM Tris-HCl, 2% (wt/vol) SDS, 10% glycerol, and 0.01% (wt/vol) bromophenol blue, heated to 95°C for 2 min and subjected to SDS-PAGE.

Online supplemental material

The images shown in Fig. S1 (A and B) demonstrate that monoclonal antibodies directed against p38^{P} present the same colocalization with keratin granules as other polyclonal antibodies (see Fig. 1). Similarly, fluorescent K18 and p38 chimeras colocalize in prominent cytoplasmic aggregates (Fig. S1, C and D). The fluorescence micrographs provided in Fig. S2 show that phosphorylation of K8-S431 is not affected by OV; those in Fig. S3 demonstrate that the keratin cytoskeleton is reorganized in response to p38 down-regulation and that K8-S73D mutation does not affect overall network formation. Fig. S4 summarizes colocalization results for keratins and specific keratin phosphoepitopes or phosphorylated p38, JNKs, and ERKs during various situations of pronounced KF network alterations. Fig. S5 lists the oligonucleotides used for cloning. Videos 1 and 2 corresponding to Fig. 10, A and B, respectively, reveal the inhibitory effects of pharmacological p38 inactivation on KF precursor formation. Video 3 further shows that p38 inhibition prevents mutant keratin granule turnover. Online supplemental material is available at http://www.jcb.org/cgi/content/full/jcb.200703174/DC1.

We thank Dr. Roger J. Davis, Dr. Cynthia A. Bradham, and Anne Kölsch for DNA constructs; Dr. Bishr Omary for DNA constructs and antibodies; Dr. Thomas Magin for cell lines; Anne Kölsch and Dr. Laurent Kreplak for helpful comments; and Ursula Wilhelm for expert technical assistance.

The work was supported by the German Research Council.

Submitted: 27 March 2007
Accepted: 4 May 2007

References

Ackerley, S., A.J. Grierson, S. Banner, M.S. Perkinton, J. Brownlees, H.L. Byers, M. Ward, P. Thornhill, K. Hussain, J.S. Waby, et al. 2004. p38alpha stress-activated protein kinase phosphorylates neurofilaments and is associated with neurofilament pathology in amyotrophic lateral sclerosis. *Mol. Cell. Neurosci.* 26:354–364.

Al-Chalabi, A., and C.C. Miller. 2003. Neurofilaments and neurological disease. *Bioessays.* 25:346–355.

Bakin, A.V., C. Rinehart, A.K. Tomlinson, and C.L. Arteaga. 2002. p38 mitogen-activated protein kinase is required for TGFbeta-mediated fibroblastic transdifferentiation and cell migration. *J. Cell Sci.* 115:3193–3206.

Bendotti, C., C. Atzori, R. Piva, M. Tortarolo, M.J. Strong, S. DeBiasi, and A. Migheli. 2004. Activated p38MAPK is a novel component of the intracellular inclusions found in human amyotrophic lateral sclerosis and mutant SOD1 transgenic mice. *J. Neuropathol. Exp. Neurol.* 63:113–119.

Berkowitz, P., P. Hu, Z. Liu, L.A. Diaz, J.J. Enghild, M.P. Chua, and D.S. Rubenstein. 2005. Desmosome signaling. Inhibition of p38MAPK prevents pemphigus vulgaris IgG-induced cytoskeleton reorganization. *J. Biol. Chem.* 280:23778–23784.

Bradham, C.A., and D.R. McClay. 2006. p38 MAPK is essential for secondary axis specification and patterning in sea urchin embryos. *Development.* 133:21–32.

Cano, E., Y.N. Doza, R. Ben-Levy, P. Cohen, and L.C. Mahadevan. 1996. Identification of anisomycin-activated kinases p45 and p55 in murine cells as MAPKAP kinase-2. *Oncogene.* 12:805–812.

Chen, W., and G.T. Bowden. 1999. Activation of p38 MAP kinase and ERK are required for ultraviolet-B induced c-fos gene expression in human keratinocytes. *Oncogene.* 18:7469–7476.

Cheng, H., J. Kartenbeck, K. Kabsch, X. Mao, M. Marques, and A. Alonso. 2002. Stress kinase p38 mediates EGFR transactivation by hyperosmolar concentrations of sorbitol. *J. Cell. Physiol.* 192:234–243.

Cheng, T.J., and Y.K. Lai. 1998. Identification of mitogen-activated protein kinase-activated protein kinase-2 as a vimentin kinase activated by okadaic acid in 9L rat brain tumor cells. *J. Cell. Biochem.* 71:169–181.

Chou, Y.H., P. Opal, R.A. Quinlan, and R.D. Goldman. 1996. The relative roles of specific N- and C-terminal phosphorylation sites in the disassembly of intermediate filament in mitotic BHK-21 cells. *J. Cell Sci.* 109:817–826.

Coulombe, P.A., and M.B. Omary. 2002. 'Hard' and 'soft' principles defining the structure, function and regulation of keratin intermediate filaments. *Curr. Opin. Cell Biol.* 14:110–122.

Coulombe, P.A., and P. Wong. 2004. Cytoplasmic intermediate filaments revealed as dynamic and multipurpose scaffolds. *Nat. Cell Biol.* 6:699–706.

D'Alessandro, M., D. Russell, S.M. Morley, A.M. Davies, and E.B. Lane. 2002. Keratin mutations of epidermolysis bullosa simplex alter the kinetics of stress response to osmotic shock. *J. Cell Sci.* 115:4341–4351.

Davies, S.P., H. Reddy, M. Caivano, and P. Cohen. 2000. Specificity and mechanism of action of some commonly used protein kinase inhibitors. *Biochem. J.* 351:95–105.

Eckert, R.L., T. Efimova, S.R. Dashti, S. Balasubramanian, A. Deucher, J.F. Crish, M. Sturniolo, and F. Bone. 2002. Keratinocyte survival, differentiation, and death: many roads lead to mitogen-activated protein kinase. *J. Investig. Dermatol. Symp. Proc.* 7:36–40.

Eckert, R.L., T. Efimova, S. Balasubramanian, J.F. Crish, F. Bone, and S. Dashti. 2003. p38 Mitogen-activated protein kinases on the body surface–a function for p38 delta. *J. Invest. Dermatol.* 120:823–828.

Efimova, T., A.M. Broome, and R.L. Eckert. 2003. A regulatory role for p38 delta MAPK in keratinocyte differentiation. Evidence for p38 delta-ERK1/2 complex formation. *J. Biol. Chem.* 278:34277–34285.

Feng, L., X. Zhou, J. Liao, and M.B. Omary. 1999. Pervanadate-mediated tyrosine phosphorylation of keratins 8 and 19 via a p38 mitogen-activated protein kinase-dependent pathway. *J. Cell Sci.* 112:2081–2090.

Fickert, P., M. Trauner, A. Fuchsbichler, C. Stumptner, K. Zatloukal, and H. Denk. 2003. Mallory body formation in primary biliary cirrhosis is associated with increased amounts and abnormal phosphorylation and ubiquitination of cytokeratins. *J. Hepatol.* 38:387–394.

Fontao, L., B. Favre, S. Riou, D. Geerts, F. Jaunin, J.H. Saurat, K.J. Green, A. Sonnenberg, and L. Borradori. 2003. Interaction of the bullous pemphigoid antigen 1 (BP230) and desmoplakin with intermediate filaments is mediated by distinct sequences within their COOH terminus. *Mol. Biol. Cell.* 14:1978–1992.

Garmyn, M., T. Mammone, A. Pupe, D. Gan, L. Declercq, and D. Maes. 2001. Human keratinocytes respond to osmotic stress by p38 map kinase regulated induction of HSP70 and HSP27. *J. Invest. Dermatol.* 117:1290–1295.

Gibb, B.J., J. Robertson, and C.C. Miller. 1996. Assembly properties of neurofilament light chain Ser55 mutants in transfected mammalian cells. *J. Neurochem.* 66:1306–1311.

Gibb, B.J., J.P. Brion, J. Brownlees, B.H. Anderton, and C.C. Miller. 1998. Neuropathological abnormalities in transgenic mice harbouring a phosphorylation mutant neurofilament transgene. *J. Neurochem.* 70:492–500.

Gibbons, I.R., A. Lee-Eiford, G. Mocz, C.A. Phillipson, W.-J.Y. Tang, and B.H. Gibbons. 1987. Photosensitized cleavage of dynein heavy chains. *J. Biol. Chem.* 262:2780–2786.

Gohara, R., D. Tang, H. Inada, M. Inagaki, Y. Takasaki, and S. Ando. 2001. Phosphorylation of vimentin head domain inhibits interaction with the carboxyl-terminal end of alpha-helical rod domain studied by surface plasmon resonance measurements. *FEBS Lett.* 489:182–186.

Harper, E.G., S.M. Alvares, and W.G. Carter. 2005. Wounding activates p38 map kinase and activation transcription factor 3 in leading keratinocytes. *J. Cell Sci.* 118:3471–3485.

Hatzfeld, M., and C. Nachtsheim. 1996. Cloning and characterization of a new armadillo family member, p0071, associated with the junctional plaque: evidence for a subfamily of closely related proteins. *J. Cell Sci.* 109:2767–2778.

He, T., A. Stepulak, T.H. Holmstrom, M.B. Omary, and J.E. Eriksson. 2002. The intermediate filament protein keratin 8 is a novel cytoplasmic substrate for c-Jun N-terminal kinase. *J. Biol. Chem.* 277:10767–10774.

Helfand, B.T., L. Chang, and R.D. Goldman. 2003. The dynamic and motile properties of intermediate filaments. *Annu. Rev. Cell Dev. Biol.* 19:445–467.

Herrmann, H., M. Hesse, M. Reichenzeller, U. Aebi, and T.M. Magin. 2003. Functional complexity of intermediate filament cytoskeletons: from structure to assembly to gene ablation. *Int. Rev. Cytol.* 223:83–175.

Hofmann, I., C. Mertens, M. Brettel, V. Nimmrich, M. Schnolzer, and H. Herrmann. 2000. Interaction of plakophilins with desmoplakin and intermediate filament proteins: an in vitro analysis. *J. Cell Sci.* 113:2471–2483.

Hofmann, M., J. Zaper, A. Bernd, J. Bereiter-Hahn, R. Kaufmann, and S. Kippenberger. 2004. Mechanical pressure-induced phosphorylation of p38 mitogen-activated protein kinase in epithelial cells via Src and protein kinase C. *Biochem. Biophys. Res. Commun.* 316:673–679.

Inagaki, M., Y. Gonda, K. Nishizawa, S. Kitamura, C. Sato, S. Ando, K. Tanabe, K. Kikuchi, S. Tsuiki, and Y. Nishi. 1990. Phosphorylation sites linked to glial filament disassembly in vitro locate in a non-alpha-helical head domain. *J. Biol. Chem.* 265:4722–4729.

Inagaki, M., Y. Matsuoka, K. Tsujimura, S. Ando, T. Tokui, T. Takahashi, and N. Inagaki. 1996. Dynamic property of intermediate filaments: regulation by phosphorylation. *Bioessays.* 18:481–487.

Izawa, I., and M. Inagaki. 2006. Regulatory mechanisms and functions of intermediate filaments: a study using site- and phosphorylation state-specific antibodies. *Cancer Sci.* 97:167–174.

Johansen, C., K. Kragballe, M. Westergaard, J. Henningsen, K. Kristiansen, and L. Iversen. 2005. The mitogen-activated protein kinases p38 and ERK1/2 are increased in lesional psoriatic skin. *Br. J. Dermatol.* 152:37–42.

Kim, S., P. Wong, and P.A. Coulombe. 2006. A keratin cytoskeletal protein regulates protein synthesis and epithelial cell growth. *Nature.* 441:362–365.

Klekotka, P.A., S.A. Santoro, and M.M. Zutter. 2001. alpha 2 integrin subunit cytoplasmic domain-dependent cellular migration requires p38 MAPK. *J. Biol. Chem.* 276:9503–9511.

Kowalczyk, A.P., M. Hatzfeld, E.A. Bornslaeger, D.S. Kopp, J.E. Borgwardt, C.M. Corcoran, A. Settler, and K.J. Green. 1999. The head domain of plakophilin-1 binds to desmoplakin and enhances its recruitment to desmosomes. Implications for cutaneous disease. *J. Biol. Chem.* 274:18145–18148.

Kreplak, L., U. Aebi, and H. Herrmann. 2004. Molecular mechanisms underlying the assembly of intermediate filaments. *Exp. Cell Res.* 301:77–83.

Ku, N.O., and M.B. Omary. 1997. Phosphorylation of human keratin 8 in vivo at conserved head domain serine 23 and at epidermal growth factor-stimulated tail domain serine 431. *J. Biol. Chem.* 272:7556–7564.

Ku, N.O., and M.B. Omary. 2006. A disease- and phosphorylation-related nonmechanical function for keratin 8. *J. Cell Biol.* 174:115–125.

Ku, N.O., S. Azhar, and M.B. Omary. 2002. Keratin 8 phosphorylation by p38 kinase regulates cellular keratin filament reorganization: modulation by a keratin 1-like disease causing mutation. *J. Biol. Chem.* 277:10775–10782.

Ku, N.O., H. Fu, and M.B. Omary. 2004. Raf-1 activation disrupts its binding to keratins during cell stress. *J. Cell Biol.* 166:479–485.

Leung, C.L., K.J. Green, and R.K. Liem. 2002. Plakins: a family of versatile cytolinker proteins. *Trends Cell Biol.* 12:37–45.

Liao, J., and M.B. Omary. 1996. 14-3-3 proteins associate with phosphorylated simple epithelial keratins during cell cycle progression and act as a solubility cofactor. *J. Cell Biol.* 133:345–357.

Liao, J., N.O. Ku, and M.B. Omary. 1997. Stress, apoptosis, and mitosis induce phosphorylation of human keratin 8 at Ser-73 in tissues and cultured cells. *J. Biol. Chem.* 272:17565–17573.

Listwan, P., and J.A. Rothnagel. 2004. Keratin bundling proteins. *Methods Cell Biol.* 78:817–827.

Lowthert, L.A., N.O. Ku, J. Liao, P.A. Coulombe, and M.B. Omary. 1995. Empigen BB: a useful detergent for solubilization and biochemical analysis of keratins. *Biochem. Biophys. Res. Commun.* 206:370–379.

Magin, T.M., P. Vijayaraj, and R.E. Leube. 2007. Structural and regulatory functions of keratins. *Exp. Cell Res.* In press.

Nan, L., J. Dedes, B.A. French, F. Bardag-Gorce, J. Li, Y. Wu, and S.W. French. 2006. Mallory body (cytokeratin aggresomes) formation is prevented in vitro by p38 inhibitor. *Exp. Mol. Pathol.* 80:228–240.

Omary, M.B., P.A. Coulombe, and W.H. McLean. 2004. Intermediate filament proteins and their associated diseases. *N. Engl. J. Med.* 351:2087–2100.

Omary, M.B., N.O. Ku, G.Z. Tao, D.M. Toivola, and J. Liao. 2006. 'Heads and tails' of intermediate filament phosphorylation: multiple sites and functional insights. *Trends Biochem. Sci.* 31:383–394.

Raingeaud, J., A.J. Whitmarsh, T. Barrett, B. Derijard, and R.J. Davis. 1996. MKK3- and MKK6-regulated gene expression is mediated by the p38 mitogen-activated protein kinase signal transduction pathway. *Mol. Cell. Biol.* 16:1247–1255.

Rezniczek, G.A., L. Janda, and G. Wiche. 2004. Plectin. *Methods Cell Biol.* 78:721–755.

Ridge, K.M., L. Linz, F.W. Flitney, E.R. Kuczmarski, Y.H. Chou, M.B. Omary, J.I. Sznajder, and R.D. Goldman. 2005. Keratin 8 phosphorylation by protein kinase C delta regulates shear stress-mediated disassembly of keratin intermediate filaments in alveolar epithelial cells. *J. Biol. Chem.* 280:30400–30405.

Schweizer, J., P.E. Bowden, P.A. Coulombe, L. Langbein, E.B. Lane, T.M. Magin, L. Maltais, M.B. Omary, D.A. Parry, M.A. Rogers, and M.W. Wright. 2006. New consensus nomenclature for mammalian keratins. *J. Cell Biol.* 174:169–174.

Sharma, G.D., J. He, and H.E. Bazan. 2003. p38 and ERK1/2 coordinate cellular migration and proliferation in epithelial wound healing: evidence of cross-talk activation between MAP kinase cascades. *J. Biol. Chem.* 278:21989–21997.

Smith, E.A., and E. Fuchs. 1998. Defining the interactions between intermediate filaments and desmosomes. *J. Cell Biol.* 141:1229–1241.

Steinbock, F.A., B. Nikolic, P.A. Coulombe, E. Fuchs, P. Traub, and G. Wiche. 2000. Dose-dependent linkage, assembly inhibition and disassembly of vimentin and cytokeratin 5/14 filaments through plectin's intermediate filament-binding domain. *J. Cell Sci.* 113:483–491.

Stoll, S.W., S. Kansra, and J.T. Elder. 2003. Keratinocyte outgrowth from human skin explant cultures is dependent upon p38 signaling. *Wound Repair Regen.* 11:346–353.

Strnad, P., R. Windoffer, and R.E. Leube. 2002. Induction of rapid and reversible cytokeratin filament network remodeling by inhibition of tyrosine phosphatases. *J. Cell Sci.* 115:4133–4148.

Strnad, P., R. Windoffer, and R.E. Leube. 2003. Light-induced resistance of the keratin network to the filament-disrupting tyrosine phosphatase inhibitor orthovanadate. *J. Invest. Dermatol.* 120:198–203.

Stumptner, C., M.B. Omary, P. Fickert, H. Denk, and K. Zatloukal. 2000. Hepatocyte cytokeratins are hyperphosphorylated at multiple sites in human alcoholic hepatitis and in a Mallory body mouse model. *Am. J. Pathol.* 156:77–90.

Takemura, M., H. Gomi, E. Colucci-Guyon, and S. Itohara. 2002. Protective role of phosphorylation in turnover of glial fibrillary acidic protein in mice. *J. Neurosci.* 22:6972–6979.

Tao, G.Z., Q. Zhou, P. Strnad, M.R. Salemi, Y.M. Lee, and M.B. Omary. 2005. Human Ran cysteine 112 oxidation by pervanadate regulates its binding to keratins. *J. Biol. Chem.* 280:12162–12167.

Tao, G.Z., D.M. Toivola, Q. Zhou, P. Strnad, B. Xu, S.A. Michie, and M.B. Omary. 2006. Protein phosphatase-2A associates with and dephosphorylates keratin 8 after hyposmotic stress in a site- and cell-specific manner. *J. Cell Sci.* 119:1425–1432.

Toivola, D.M., Q. Zhou, L.S. English, and M.B. Omary. 2002. Type II keratins are phosphorylated on a unique motif during stress and mitosis in tissues and cultured cells. *Mol. Biol. Cell.* 13:1857–1870.

Toivola, D.M., N.O. Ku, E.Z. Resurreccion, D.R. Nelson, T.L. Wright, and M.B. Omary. 2004. Keratin 8 and 18 hyperphosphorylation is a marker of progression of human liver disease. *Hepatology.* 40:459–466.

Tortarolo, M., P. Veglianese, N. Calvaresi, A. Botturi, C. Rossi, A. Giorgini, A. Migheli, and C. Bendotti. 2003. Persistent activation of p38 mitogen-activated protein kinase in a mouse model of familial amyotrophic lateral sclerosis correlates with disease progression. *Mol. Cell. Neurosci.* 23:180–192.

van de Wetering, M., I. Oving, V. Muncan, M.T. Pon Fong, H. Brantjes, D. van Leenen, F.C. Holstege, T.R. Brummelkamp, R. Agami, and H. Clevers. 2003. Specific inhibition of gene expression using a stably integrated, inducible small-interfering-RNA vector. *EMBO Rep.* 4:609–615.

Werner, N.S., R. Windoffer, P. Strnad, C. Grund, R.E. Leube, and T.M. Magin. 2004. Epidermolysis bullosa simplex-type mutations alter the dynamics of the keratin cytoskeleton and reveal a contribution of actin to the transport of keratin subunits. *Mol. Biol. Cell.* 15:990–1002.

Wery-Zennaro, S., J.L. Zugaza, M. Letourneur, J. Bertoglio, and J. Pierre. 2000. IL-4 regulation of IL-6 production involves Rac/Cdc42- and p38 MAPK-dependent pathways in keratinocytes. *Oncogene.* 19:1596–1604.

Wilhelmsen, K., S.H. Litjens, I. Kuikman, N. Tshimbalanga, H. Janssen, I. van den Bout, K. Raymond, and A. Sonnenberg. 2005. Nesprin-3, a novel outer nuclear membrane protein, associates with the cytoskeletal linker protein plectin. *J. Cell Biol.* 171:799–810.

Windoffer, R., and R.E. Leube. 1999. Detection of cytokeratin dynamics by time-lapse fluorescence microscopy in living cells. *J. Cell Sci.* 112:4521–4534.

Windoffer, R., and R.E. Leube. 2001. De novo formation of cytokeratin filament networks originates from the cell cortex in A-431 cells. *Cell Motil. Cytoskeleton.* 50:33–44.

Windoffer, R., and R.E. Leube. 2004. Imaging of keratin dynamics during the cell cycle and in response to phosphatase inhibition. *Methods Cell Biol.* 78:321–352.

Windoffer, R., S. Wöll, P. Strnad, and R.E. Leube. 2004. Identification of novel principles of keratin filament network turnover in living cells. *Mol. Biol. Cell.* 15:2436–2448.

Windoffer, R., A. Kolsch, S. Woll, and R.E. Leube. 2006. Focal adhesions are hotspots for keratin filament precursor formation. *J. Cell Biol.* 173:341–348.

Wöll, S., R. Windoffer, and R.E. Leube. 2005. Dissection of keratin dynamics: different contributions of the actin and microtubule systems. *Eur. J. Cell Biol.* 84:311–328.

Zatloukal, K., C. Stumptner, A. Fuchsbichler, P. Fickert, C. Lackner, M. Trauner, and H. Denk. 2004. The keratin cytoskeleton in liver diseases. *J. Pathol.* 204:367–376.

Zheng, Y.L., B.S. Li, Veeranna, and H.C. Pant. 2003. Phosphorylation of the head domain of neurofilament protein (NF-M): a factor regulating topographic phosphorylation of NF-M tail domain KSP sites in neurons. *J. Biol. Chem*. 278:24026–24032.